SPE
Society of Petroleum Engineers of AIME

# MULTIPLE FRACTURING EXPERIMENTS--PROPELLANT AND BOREHOLE CONSIDERATIONS

CONF - 820524-5
MASTER

by Jerry F. Cuderman, Sandia National Laboratories

SAND--81-2224C

DE82 008179

## ABSTRACT

The technology for multiple fracturing of a wellbore, using progressively burning propellants, is being developed to enhance natural gas recovery. Multiple fracturing appears especially attractive for stimulating naturally fractured reservoirs such as Devonian shales where it is expected to effectively intersect existing fractures and connect them to a wellbore.

Previous experiments and modeling efforts[1-5] defined pressure risetimes required for multiple fracturing as a function of borehole diameter, but identified only a weak dependence on peak pressure attained. Typically, from four to eight equally spaced major fractures occur as a function of pressure risetime and in situ stress orientation.

The present experiments address propellant and rock response considerations required to achieve the desired pressure risetimes for reliable multiple fracturing.

## INTRODUCTION

Experiments at the Nevada Test Site (NTS) have demonstrated the existence of three distinct fracture regimes.[1-3,6] Depending on the pressure risetime in a borehole, one can obtain hydraulic, multiple, or explosive fracture behavior. The use of propellants, rather than explosives, in tamped boreholes permits tailoring of the pressure risetime over a wide range, since propellants having a wide range of propellant burn rates are available. This technique of using propellant combustion gases, from a full bore charge, to produce controlled borehole pressurization is termed "High Energy Gas Fracturing" (HEGF).

Several series of HEGF[1-3,6] experiments have been conducted in a tunnel complex at NTS where mineback permitted direct observation of fracturing obtained. Experiments and modeling have been conducted for borehole sizes from 0.032 m (1.25 in) diameter to 0.20 m (8 in) diameter. These resulted in a consistent set of predictions of pressure risetime requirements as a function of borehole diameter. However, the experimental data showed that while the fracturing behavior which occurred for a measured experiment pressure pulse was consistent with predictions, the pulse obtained was not necessarily that designed for the experiment. There was an apparent spread in risetimes and peak pressures for similar though not identical experiments.

Thus a series of small scale experiments (designated GFSE#3) was designed to compare shot-to-shot variation for identical experiments in different boreholes and for successive shots in the same borehole. Two military surplus, M5 large gun propellants, designated M5(A) and M5(B), were used which bracket burn rates necessary for multiple fracture in most rock types of interest. The identical experiments in different boreholes were designed to establish shot-to-shot variability, those of successive shots in the same borehole were to determine the effect of damage caused in previous shots and variation of free volume on the resulting pressure pulse.

A related experiment (GFSE#5) was designed for a 0.100 m (4 in) diameter borehole to obtain data for a borehole size intermediate between small scale experiments such as GFSE#3 and previous experiments in 0.200 (8 in) and 0.150 m (6 in) diameter boreholes. It used a mixture of M5(A) and M5(B) propellants. The objective of the mixture was (1) to obtain data relating the risetime obtained with the mixture to the risetimes of its constituents, and (2) to obtain data relating risetime for this size borehole both with the 0.048 m (1.89 in) diameter boreholes and the previous larger experiments.

Data from previous experiments will be used to complement those of GFSE #3 and GFSE #5 where appropriate.

## THEORY OF MULTIPLE FRACTURING

Considerable progress has been made in the understanding of multiple fracture behavior since the verification of the hypothesis that multiple fracturing might result from "intermediate" pressure

References and illustrations at end of paper.

rates.[4,5,7] Specifically, given peak pressure, pressure risetime, principal in situ stresses, and material properties, the modeling can predict the type of fracture obtained and fracture lengths. Clearly this is more difficult to do a priori than after the fact, when the actual pressure profile is known. However, several generalizations can be extracted from the data which enhance the modeling predictive capability. These include, for ashfall tuff:

(1) Hydraulic type fracture occurs for pressure risetimes in the range of 1-10 msec depending on borehole diameter.

(2) Multiple fracture occurs for pressure risetimes ranging from 0.05 to 5 msec depending on borehole diameter.

(3) Peak pressures for hydraulic type fracture are about 50 MPa (7000 psi).

(4) Peak pressures for optimum multiple fracture (near the multiple-explosive boundary) are about 250 MPa (36000 psi).

(5) Propellant M5(A) produces ~ 0.1 msec risetimes in 0.048 m (1.89 in) diameter boreholes; propellant M5(B) 5 msec risetimes. Pulse risetime can be tailored empirically, by mixing the two propellants to obtain risetimes intermediate between them.

Specific achievements of the modeling effort include:

(1) The multiple fracture regime is defined by the following semi-empirical criterion[4,5] as a function of Rayleigh wave velocity $C_R$, pressure risetime $t_m$ and borehole diameter D:

$$\frac{C_R}{8\pi} < \frac{D}{t_m} < \frac{2C_R}{\pi} \qquad (1)$$

For a material whose Poisson ratio is 0.3, $C_R = 0.5\ C_p$, where $C_p$ is the compressive wave velocity. It was noted,[5] in examining results from elastic wave modeling of dynamically pressurized boreholes, that the onset of borehole crushing appears to occur when the risetime $t_m = \pi D/C_p$, or more precisely, $\pi D/2C_r$. The latter result was subsequently derived analytically.[5] The lower bound for multiple fracturing was obtained by assuming the same $D/t_m$ scaling dependence but with the constant adjusted to fit existing data from 0.15 m and 0.20 m diameter boreholes.

(2) Development of a finite element model[7] which uses a tensile failure criterion and incorporates in situ principal stresses and fracture pressurization. Its predictive capabilities include type of fracture obtained, fracture length, fracture orientation, and stress and displacement as a function of borehole pressure, fracture pressure, pressure risetime, in situ stresses, and material properties.

(3) Investigation of effect of in situ stress. Like hydraulic fracture, multiple fracturing behavior appears governed by the principal in situ stresses. Major fractures generally occur radially from a wellbore along principal planes of stress. This observation has been verified by finite element modeling.[7] An additional major fracture also usually occurs in each of the quadrants defined by the intersection of the principal planes of stress.[5] This is also predicted by finite element modeling. The modeling further predicts that the fracturing is relatively insensitive to magnitude or differences in principal stresses. However, it appears crucial that there be either a difference in the horizontal principal stresses intersecting a vertical borehole or a variation in material strength around the borehole circumference.

## EXPERIMENTAL HARDWARE AND TEST ENVIRONMENT

In situ experiments to test concepts and develop hardware are conducted in a tunnel complex at NTS.[2,3,6] The experiments are done in this tunnel complex and location for several reasons. First, mineback can be done to observe fracturing results; second, the homogeneity of the beds and presence of realistic in situ stress fields, results in a nearly ideal test bed to evaluate modeling and fracture behavior, and, third, although the ash fall material properties differ considerably from those of Devonian shales, modeling efforts indicate that only relatively small adjustments in pressure rates should be required for experiments in Devonian shale.

Experiments of 0.100 m diameter or larger are emplaced from an existing drift at a 12 m depth and stemmed with wet sand. A mineback drift is subsequently extended to expose the fractured zones. Smaller "Scale Experiments" are emplaced in the end face of a drift and stemmed with sand. These experiments are typically at 3 meter total depths. Figure 1 is a schematic of the borehole configuration used in the small scale experiments. For each individual test, a 0.10 m or 0.15 m diameter ($D_o$) borehole is drilled almost horizontally to a depth $L_o$. Then a smaller borehole, usually of 0.048 m diameter D is drilled concentrically to a depth $L_1$, usually 1 m. Boreholes A, B, C, and D contain propellant canister-pressure transducer assemblies. Borehole E contains stress and acceleration instrumentation. The end of the scale experiment drift contains nearly homogeneous layers of two different kinds of tuff. The upper half of the drift face, in which the A and C experiment boreholes are drilled, is a porous, yellow, peralkaline tuff, with permeability typically in the $10^{-1}$ md range. The lower half is a competent, red tuff of about $10^{-2}$ md permeability. However, the mechanical properties, listed in Table 1, are the same for both.

The canister assembly developed for the in situ experiments,[6] used in GFSE #3, consists of a PVC propellant canister attached to a pressure transducer assembly. Two exploding bridge wire initiators are installed 0.3 m from each end. The initiator cables and pressure transducer cables are brought out of the borehole through a pipe attached to the back of the pressure transducer units.

The experiment canister for GFSE #5 used the same pressure transducer assembly. It was also of PVC construction, but employed a centralized Rapid Ignition Propagation ignitor. This ignitor, when initiated at one end with an exploding bridge wire, ignites the entire length of the canister simultaneously.

Two types of propellants were used in these experiments. Their descriptions appear in Table 2. Both are M5-type. The smaller propellant M5(A) produces pulses whose risetimes are less than 1 msec in small boreholes. The use of the larger grains M5(B) produces pressure risetimes of several msec in 0.048 m (1.89 in) diameter boreholes.[6] Prior to experiment installation, the borehole transmissivities were measured using both constant pressure injection and shut-in tests.

After experiment insertion, wet Overton, Nevada sand was mechanically tamped to fill the borehole. A short plug of a fast setting, sulfur-based cement mixed with sand and water, was ordinarily set in the collar. This served to contain the propellant burn and retain the experiment and sand in the borehole.

A number of experiments were done in test series GFSE #3 to compare data scatter as a function of propellant and borehole condition. Referring again to Figure 1, a single experiment was done in borehole A, while two successive identical experiments were conducted in B. The propellant used in the Borehole A and B shots was M5(A). Similarly, only one experiment was done in Borehole C and four in Borehole D with M5(B) propellant. For the fourth experiment in D, the free volume around the canister was eliminated by filling with water. The single shot data from A and C not only permits a comparison between single and multiple shot results, but results in an evaluation of the effect of material change, since the tuff in the top half of the drift face is more porous than that below it.

The canister used in the GFSE #5 experiment was first tested in a 90 mm army surplus cannon using M5(B) propellant. A 0.3 m (1 ft) long wet sand tamp at each end of the canister contained the burn to 345 MPa (50,000 psi). It achieved the 250 MPa (36,000 psi) pressure, where multiple fracturing is observed to occur, in 1.25 msec. Since there was essentially no annular free volume around the canister in the 90 mm cannon, this risetime is faster than would occur in a 0.10 m diameter borehole. A 2 msec risetime is estimated for straight M5(B) propellant in a 0.10 (4 in) diameter borehole. On the basis of previous tests, a 25% M5(A)/75% M5(B) mixture, by weight, was specified for a 0.5 msec risetime.

## DATA AND RESULTS

Figure 2 presents the pressure waveforms obtained for the slower of the two propellants, M5(B). These experiments were done in boreholes C and D. (The number after the borehole designation denotes the shot number; for example, GFSE #3D2 refers to the second shot in borehole D in experiment GFSE #3.) In each case there is an initial pressure rise followed by a decrease of several msec duration. The pressure then continues to rise to a maximum and subsequently decays. A borehole tv scan after each test revealed hydraulic type fracture. It appears likely that the break in the pressure rise coincides with fracture formation. The origin of the high frequency noise imposed on the pulse is unknown. It may be due to pressure wave phenomena in the borehole or to excitation of a resonance in the gage, although tests show its response is linear into the microsecond regime.

It is seen that there is a factor of three difference in peak pressure between identical first shots in three different boreholes. However, for successive shots in the same borehole, the amplitudes are essentially identical except for shot 4, where the hole was backfilled with water to reduce free volume. The presence of water in the borehole resulted in a decrease in pressure risetime to 2 msec from the 5 to 8.5 seen in the preceding shots. It also attenuated the peak pressure attained by about a factor of two.

Figure 3 presents the pressure records from the 0.048 m (1.89 in) diameter boreholes A and B of GFSE #3. The faster M5-A propellant was used in these tests. Typical risetimes are a few tenths of a msec to the "apparent" peak pressure. Expanded records show that the pulses have superimposed upon them a ringing frequency of 0.1 to 0.15 msec periodicity as did those of experiments C and D. However, here it is more serious, since it cuts off the pressure rise in a few tenths of a msec or less and makes identification of the true risetime and peak pressure difficult if not impossible. In A1 and B2, the signal goes negative at 0.1 and 0.2 msec respectively. A pressure drop of 110 MPa in 0.1 msec is unlikely, since fractures sufficient to relieve that much pressure in such a short time are improbable. Therefore the "apparent" peak pressures should be regarded as lower bounds. This is also true of B1 even though it did not go negative, but suffered a pressure drop from 158 MPa (23000 psi) to 100 MPa(14000 psi) in less than 0.1 msec at 0.2 msec into the pulse.

Because of the high frequency oscillations, it is not clear whether the observed large difference in peak amplitudes for shots A1 and B1 is real. It is noted that the pressure decay, starting 3 msec after the start of the initial pressure rise, is only slightly less for A1 than for B1. The difference between B1 and B2, however, appears significant. A tv log of the borehole after shot B1 revealed a highly multiple fractured borehole condition.

This conclusion was further supported by a transmissivity increase from $5 \times 10^{-2}$ md before the test to 1.93 md post test. Measurement of transmissivity after shot B2, however, showed a decrease to 0.96 md. Both the decrease in transmissivity and the 0.04 msec apparent risetime suggest that shot B2 produced a crushed borehole. The GFSE #5 experiment, designed to produce a 250 MPa (36,000 psi) peak pressure with a 0.5 msec risetime yielded a 258 MPa (37,500 psi) peak pressure at a 0.56 msec risetime.

Table 3 summarizes both the data obtained in the present experiments and those which are appropriate from previous series for comparison with results of the present experiments.

## INTERPRETATION OF DATA

Figure 4 is a plot of the boundaries of multiple, hydraulic, and explosive fracture as defined by Eq. (1) in terms of borehole diameter, D, and pressure risetime $t_m$. Essentially all the experimental data points to date appear on Fig. 4. Those indicated only as A1, B2, C1...on this and succeeding figures are all from GFSE #3. The fractures from experiments GFSE #5 and B2 and D4 have not yet been visually verified by borehole tv scans or mineback. However, from the post test increase in transmissivity, GFSE #5 is almost certainly multiple. Likewise, transmissivity as well as the risetime data identify D4 and B2 as hydraulic and explosive type fractures, respectively. Thus, for some 21 fracture experiments to date there does not appear to be a single exception to the fracture type obtained and that predicted by the semiempirical model in terms of borehole diameter and pressure risetime.

A possible explanation for the apparent crushed borehole result of B2 is that Shot B1 left the fractures propped open and the borehole surroundings highly stressed. A second shot, B2, could thus superimpose sufficient additional stress to cause crushing.

Figure 5 is a log-log plot of peak pressure vs pressure risetime. The data points on Fig. 5, as can be checked in Table 3, are plotted without regard to borehole size. The data spread for the dry hydraulic fracture type experiments extends from 30-100 MPa and from 5-8.5 msec in risetime, and is even greater when one includes D4. The reasons for this large scatter may include small differences in free volume, rock properties, material inhomogeneities, propellant packing density, and small natural fractures. In any event such small perturbations or combinations of them is expected to result in a greater data spread for small boreholes than for large ones. Thus, the nearly horizontal part of the curve in Fig. 5 was drawn with a bias toward the data of GF 1, 5, 6, and 8 and is still consistent with the small borehole results. The implication of the data plotted in Fig. 5 is that the peak pressure is independent of borehole radius and is determined strictly by the pressure risetime.

Figure 6 is a plot of borehole size vs pressure risetime on which are plotted available data points for the M5(A) and M5(B) propellants. Since the risetime for GF8 was determined to be "less than 0.02 msec," the curve for M5(A) was arbitrarily drawn through 0.01 msec for a 0.200 m diameter to make it parallel to that of M5(B). Figure 6 graphically illustrates the difficulty of specifying a propellant for a desired risetime. A factor of 10 difference in risetime appears to occur between the two propellants for the same borehole size. Similarly, a factor of 10 difference in risetime appears to occur for the same propellant for boreholes ranging in size between 0.05 m and 0.15 m.

A method is proposed, using the GFSE #5 data and Fig. 6 for specifying a propellant mixture for a given pressure risetime and borehole size. It is noted that for a constant borehole diameter in Fig. 6, the risetime varies logarithmically from one propellant to the other. It is therefore suggested that the logarithm of the desired risetime $t_m$, obtained from a mixture of two propellants of risetime $t_A$ and $t_B$ can be expressed as a linear combination of their logarithms weighted by their mass fractions:

$$\log t_m = K f_A \log t_A + (1 - f_A) \log t_B \qquad (2)$$

where

- $t_m$ = the desired pressure risetimes
- $f_A$ = mass fraction of propellant M5(A)
- $t_A$ = risetime if borehole filled with M5(A)
- $t_B$ = risetime if borehole filled with M5(B)
- $K$ = calibration fraction (obtained by substituting GFSE #5 experimental data)

Solving for $f_A$ and using the GFSE #5 data, one obtains:

$$f_A = \frac{\log \frac{t_m}{t_B}}{1.8 \log \frac{t_A}{t_B}} \qquad (3)$$

## CONCLUSIONS

The experiments described in this paper focused on the problems of shot-to-shot variability and the selection of propellants for multiply fracturing a wellbore. Factors of 1.7 and 3 were shown to occur as shot-to-shot variations in pressure risetime and peak pressure, respectively, for M5(B) propellant. The results for M5(A) propellant were inconclusive because of high frequency oscillations in the pressure record.

The multiple fracturing data, to date, displayed in Figures 4, 5, and 6, indicate that the critical parameters are the logarithms of $t_m$ and $P_m$ and not their absolute values. Thus, factors of 2 or 3, or more, in shot-to-shot variability of $P_m$ and $t_m$ do not seriously affect the ability to design a multiple fracture experiment.

Data from previous experiments,[2,3,6] established the specification of pressure pulse characteristics ($t_m$, $P_m$) required for multiple fracturing (Figures 4, 5). The present data permit a specification of propellants for obtaining the required pulse (Figures 5, 6). More specifically, Figure 4, or its equivalent for another rock type, allows selection of a risetime $t_m$ for optimal multiple fracturing as a function of borehole size. Given the risetime, Figure 5 gives the expected peak pressure. The loading rate required for more detailed finite element modeling, is approximated by $P_m/t_m$. Figure 6, for a given borehole size, yields the risetimes expected for each of the two available propellants if used alone. If the required risetime is intermediate between them, a mixture of the two is needed. In that case, Eq. (3) should give the fraction of M5(A), by weight, needed to produce the required risetime $t_m$.

## ACKNOWLEDGMENTS

Useful discussions with D. A. Northrop, N. R. Warpinski, J. A. Clark, and D. V. Swenson are gratefully acknowledged. A large number of individuals in Sandia National Laboratories' Field Engineering Directorate contributed to the success of the field experiments. These include J. T. McIlmoyle, Field Experiment project leader; P. W. Cooper, explosives consultation; A. C. Arthur, Mechanical Design; and M. E. Burke, Data Acquisition. This investigation was sponsored by the Gas Research Institute under the program management of J. C. Sharer.

## NOMENCLATURE

$C_p$ = Compressive wave velocity (m/sec)
$C_r$ = Rayleigh wave velocity (m/sec)
D = Borehole diamter (m)
$f_A$ = Mass fraction of M5(A) propellant
K = Calibration factor obtained by using GFSE #5 data in Eq. (2)
$P_m$ = Peak pressure occurring during propellant burn
$t_A$ = Risetime to peak pressure using propellant M5(A) for a given borehole size
$t_B$ = Risetime to peak pressure using propellant M5(B) for a given borehole size
$t_m$ = Risetime to peak pressure occurring during a given propellant burn.

## REFERENCES

1. Warpinski, N. R., Schmidt, R. A., Cooper, P. W., Walling, H. C., and Northrop, D. A., "High-Energy Gas Frac: Multiple Fracturing in a Wellbore," Proceedings of 20th U.S. Symposium on Rock Mechanics, Austin, TX (1979).

2. Schmidt, R. A., Warpinski, N. R., and Cooper, P. W., "In Situ Evaluation of Several Tailored Pulse Well Shooting Concepts," Proceedings 1980 SPE/DOE Symposium on Unconventional Gas Recovery, Pittsburgh, PA May 18-21, 1980.

3. Schmidt, R. A., et al, "Multi-Frac Final Report," SAND81-1239, Sandia National Laboratories, November, 1978.

4. Chen, E. P., "Transient Stress Analysis of High Energy Gas Fracture Experiments," Sandia National Laboratories Report, SAND81-0703, May 1981.

5. Cuderman, J. F., "Design and Modeling of Small Scale Multiple Fracturing Experiments," Sandia National Laboratories Report," SAND81-1398, December 1981.

6. Cuderman, J. F., Cooper, P. W., Northrop, D. A., in Proc. 1981 International Gas Research Conf., September 28-October 1, 1981, Los Angeles, CA.

7. Swenson, D. V., Memo to J. F. Cuderman, Sandia National Laboratories, October 21, 1981.

TABLE 1

ASHFALL TUFF MATERIAL PROPERTIES

| | |
|---|---|
| Density | 1.8 $gm/cm^3$ (112 $lb/ft^3$) |
| Porosity (Water filled) | 40% |
| Elastic Modulus | 5 GPa ($7.25x10^5$ psi) |
| Compressional Wave Velocity | 2100 m/sec (6900 ft/sec) |
| Shear Wave Velocity | 1200 m/sec (3900 ft/ sec) |
| Tensile Strength | 700 kPa (100 psi) |
| Compressive Strength (Unconfined) | 30 MPa (4350 psi) |
| Fracture Toughness | 400 kPa $\sqrt{m}$ (105 psi $\sqrt{ft}$) |

TABLE 2.

PROPELLANT DESCRIPTION

| Item | M5(A) | M5(B) |
|---|---|---|
| Grain Diameter | 1.397 mm (0.055 in) | 5 mm (0.197 in) |
| Grain Length | 6.731 mm (0.265 in) | 11 mm (0.433 in) |
| Perf. Diameter | 0.330 mm (0.13 in) | 0.50 mm (0.019 in) |
| # Perfs | 1 | 7 |
| Density | 1.66 $gm/cm^3$ (0.06 $lb/in^3$) | 1.66 $gm/cm^3$ (0.06 $lb/in^3$) |

TABLE 3. SUMMARY OF DATA USED IN EXPERIMENT ANALYSIS

| Experiment | | Borehole Dia. m (in) | Propellant Type | $P_m$[MPa(KPsi)] | $t_m$ (msec) | Fracture Type |
|---|---|---|---|---|---|---|
| GFSE #2 (Ref. 5, 6) | C1 | 0.0889 (3.5) | 0.25 M5(A)/ 0.75 M5(B) | 86 (12.5) | 0.7 | Multiple |
| | D1 | 0.048 (1.89) | M5(B) | 36 (5.2) | 6.5 | Hydraulic |
| GFSE #3 | A1 | 0.048 (1.89) | M5(A) | 110 (16) ** | 0.1 ** | Multiple |
| | B1 | 0.048 (1.89) | M5(A) | 162 (23.5) ** | 0.2 ** | Multiple |
| | B2 | 0.048 (1.89) | M5(A) | 110 (16) ** | 0.04 ** | Explosive NV* |
| | C1 | 0.048 (1.89) | M5(B) | 100 (14.5) | 6.8 | Hydraulic |
| | D1 | 0.048 (1.89) | M5(B) | 52 (7.5) | 5.2 | Hydraulic |
| | D2 | 0.048 (1.89) | M5(B) | 48 (7) | 5.0 | Hydraulic |
| | D3 | 0.048 (1.89) | M5(B) | 48 (7) | 8.5 | Hydraulic |
| | D4 | 0.048 (1.89) | M5(B) | 28 (4) | 2.0 | Hydraulic NV* |
| GFSE #5 | -1 | 0.102 (4.00) | 0.25 M5(A)/ 0.75 M5(B) | 258 (37.5) | 0.56 | Multiple NV* |
| Multi-Frac (Ref. 5, 6) | | | | | | |
| | GF4 | 0.150 (6.00) | M5(B) | 250 (36.3) | 0.5 | Multiple |
| | GF5,6 | 0.150 (6.00) | - | 38 (5.5) | 1.0 | Multiple |
| | GF8 | 0.150 (6.00) | - | 30 (4.35) | 13 | Hydraulic |
| Gas Frac (Ref. 1) | | | | | | |
| | 1 | 0.200 (8.00) | M5 (very large grain) | 47 (6.8) | 8 | Hydraulic |
| | 2 | 0.200 (8.00) | M5(B) | 95 (14.0) | 0.7 | Multiple |
| | 3 | 0.200 (8.00) | M5(A) | ~200 (29) | < 0.02 | Explosive |

* NV--The type of fracture data and modeling would predict is listed, but Not Verified (NV), by mineback or borehole tv.

** Should be regarded only as a lower bound.

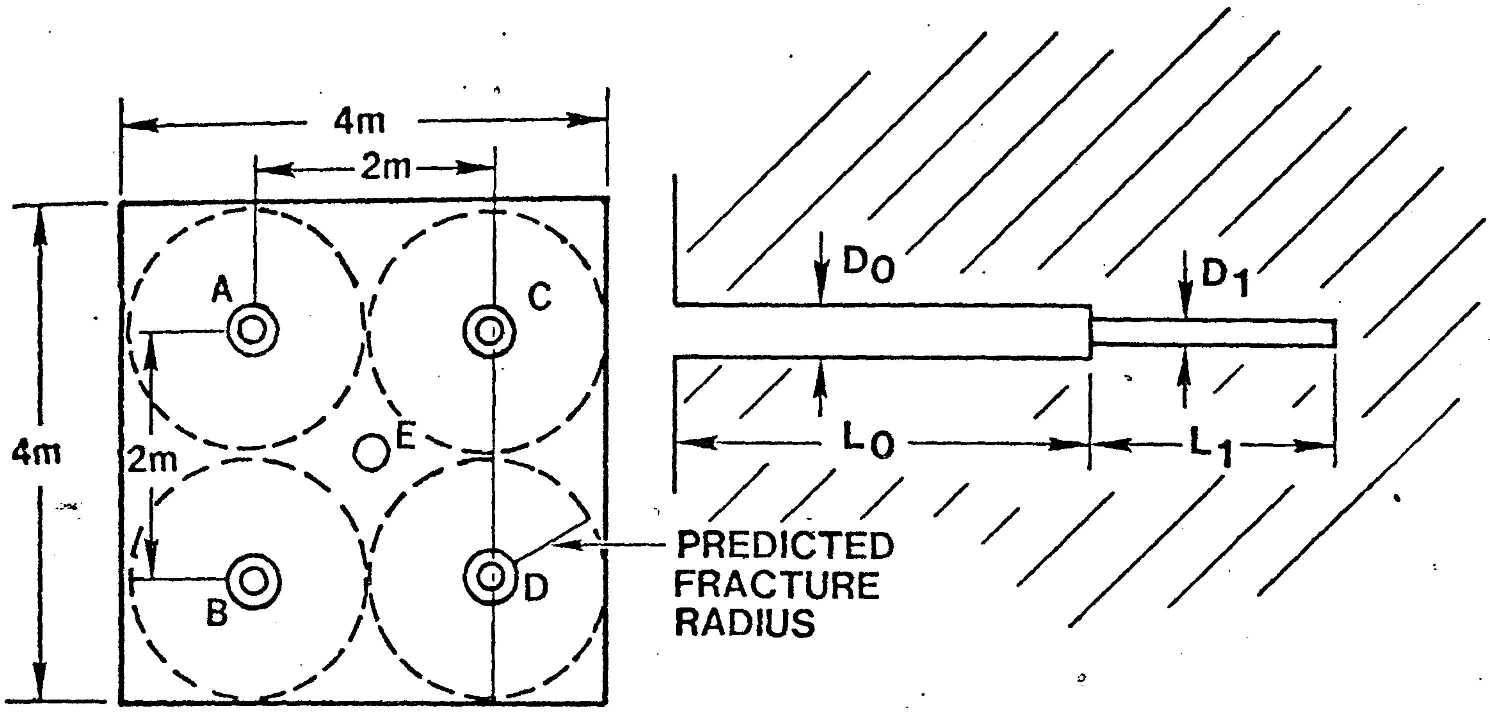


FIG 1

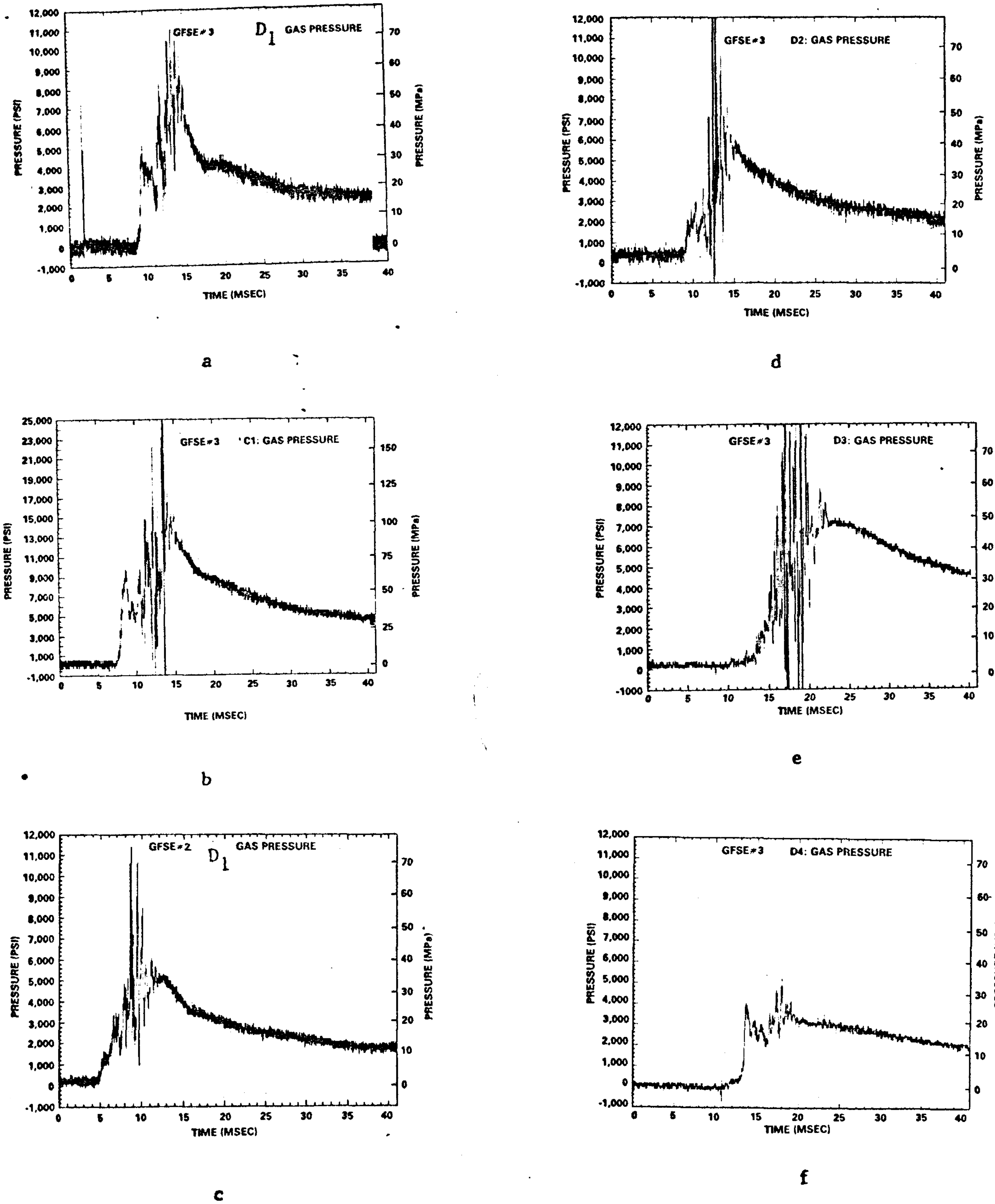


Figure 2, Pressure records for identical M5(B) propellant shots in different (a,b,c), the same(a,d,e) and water filled (f) boreholes.

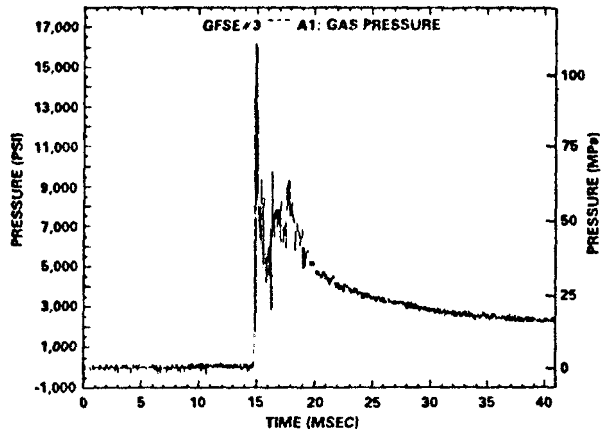


a

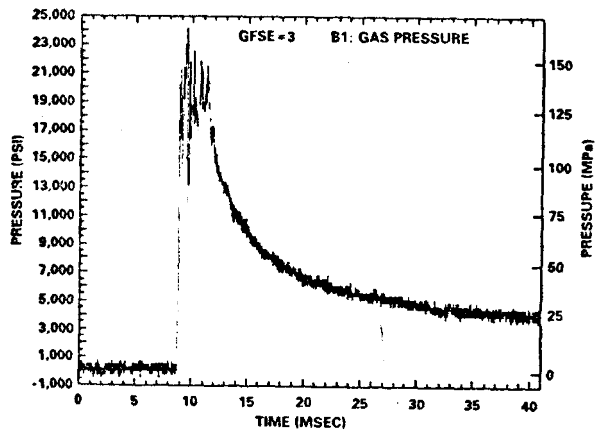


b

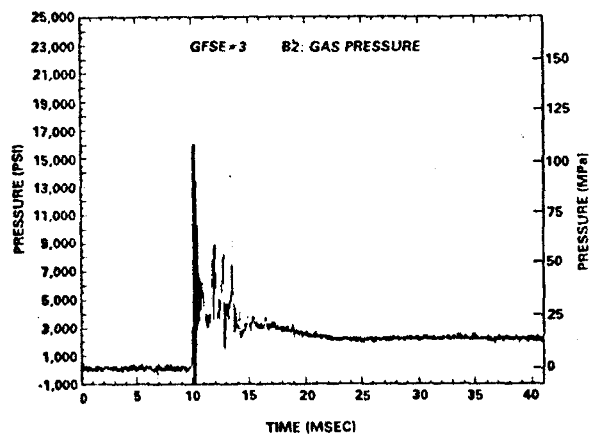


c

Figure 3 Pressure records for identical M5(A) shots in different boreholes (a,b) and the same borehole (b,c)

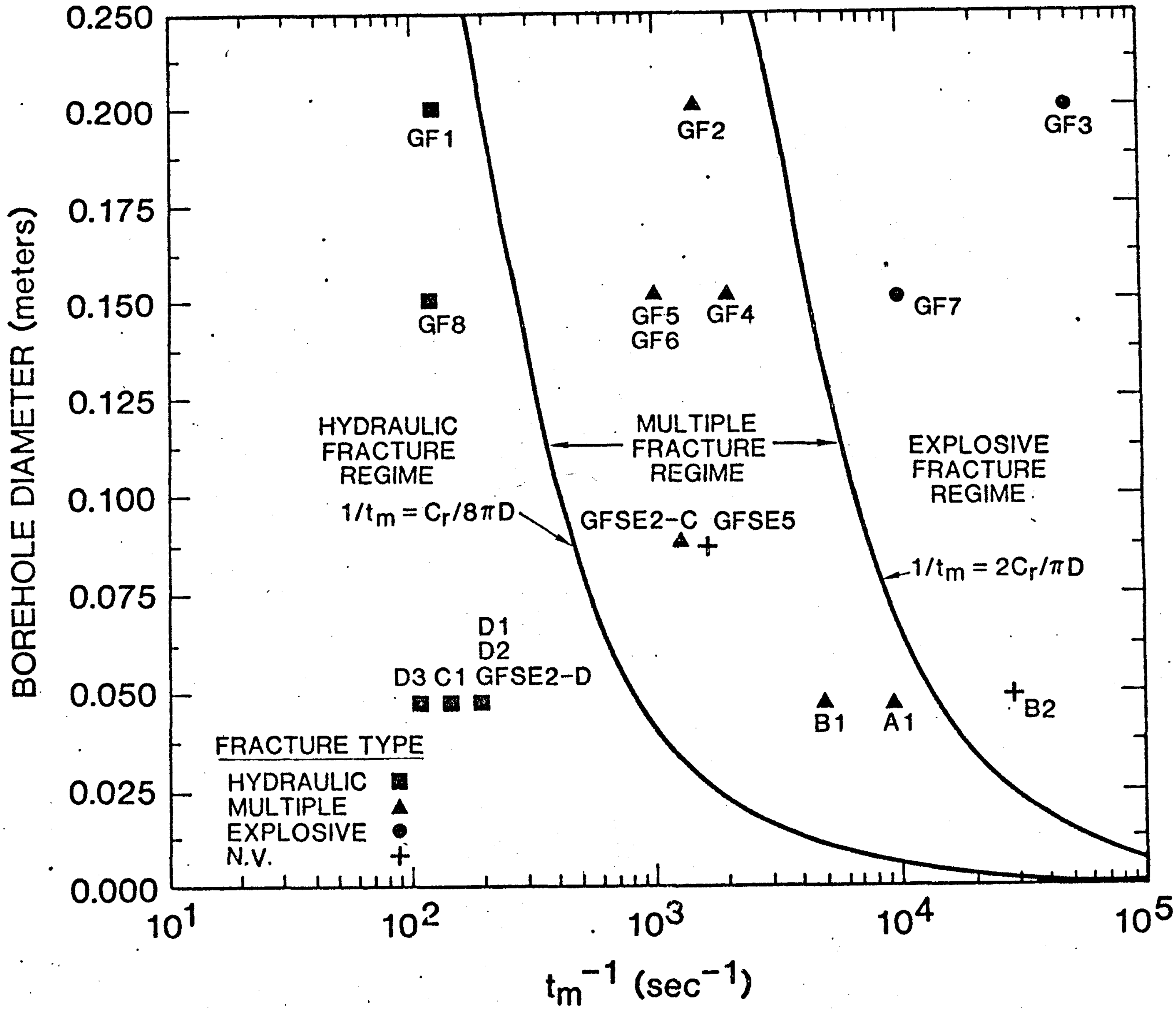
0.250
0.200
0.175
0.150
0.125
0.100
0.075
0.050
0.025
0.000
BOREHOLE DIAMETER (meters)
GF1
GF2
GF3
GF8
GF5
GF6
GF4
GF7
HYDRAULIC FRACTURE REGIME
MULTIPLE FRACTURE REGIME
EXPLOSIVE FRACTURE REGIME
1/tm = Cr/8πD
GFSE2-C GFSE5
1/tm = 2Cr/πD
D1
D2
D3 C1 GFSE2-D
B1
A1
B2
FRACTURE TYPE
HYDRAULIC
MULTIPLE
EXPLOSIVE
N.V.
10^1
10^2
10^3
10^4
10^5
tm^-1 (sec^-1)

FIG 4

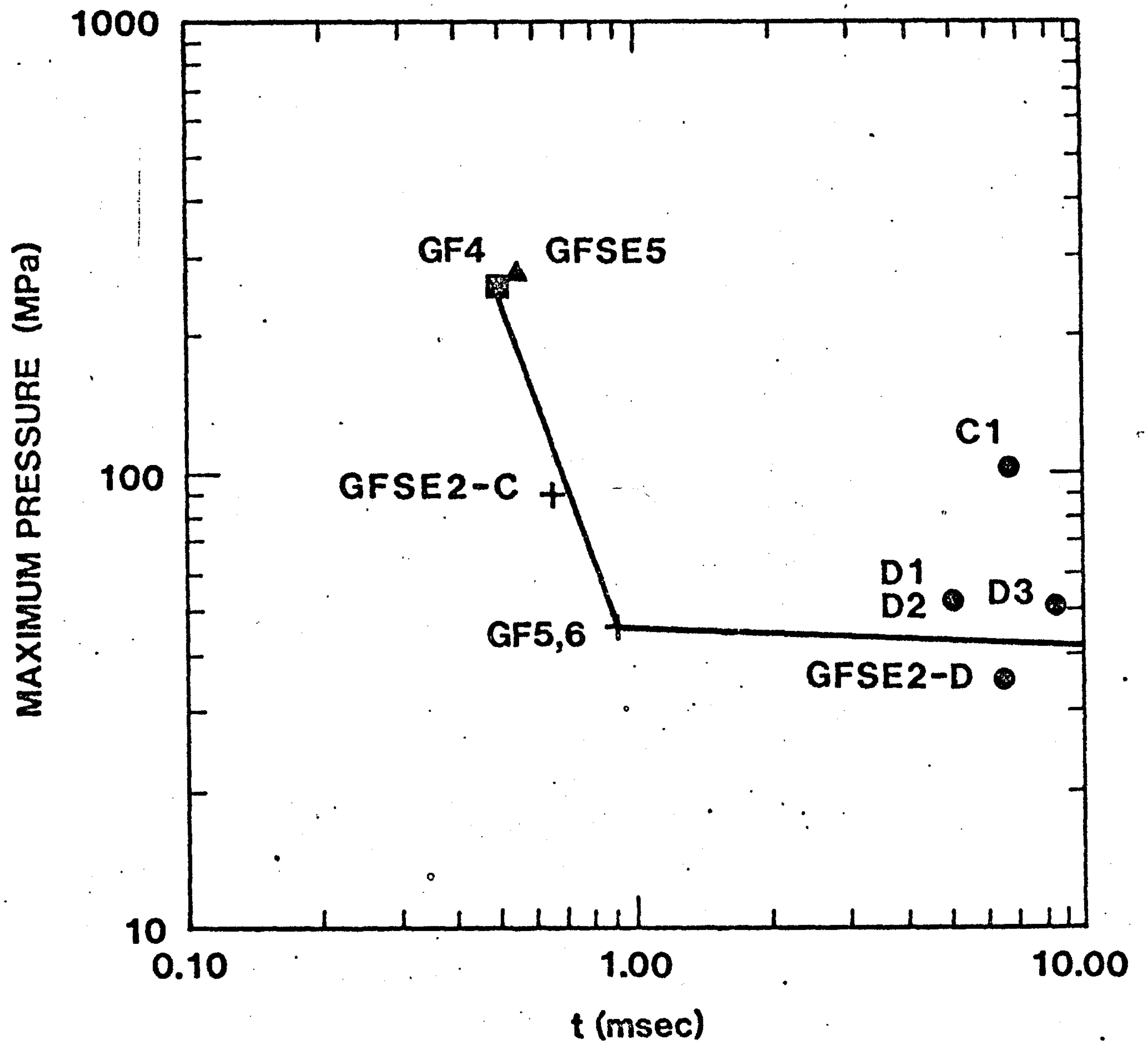
1000
100
10
MAXIMUM PRESSURE (MPa)
0.10
1.00
10.00
t (msec)
GF4
GFSE5
GFSE2-C
GF5,6
C1
D1
D2
D3
GFSE2-D

FIG 5

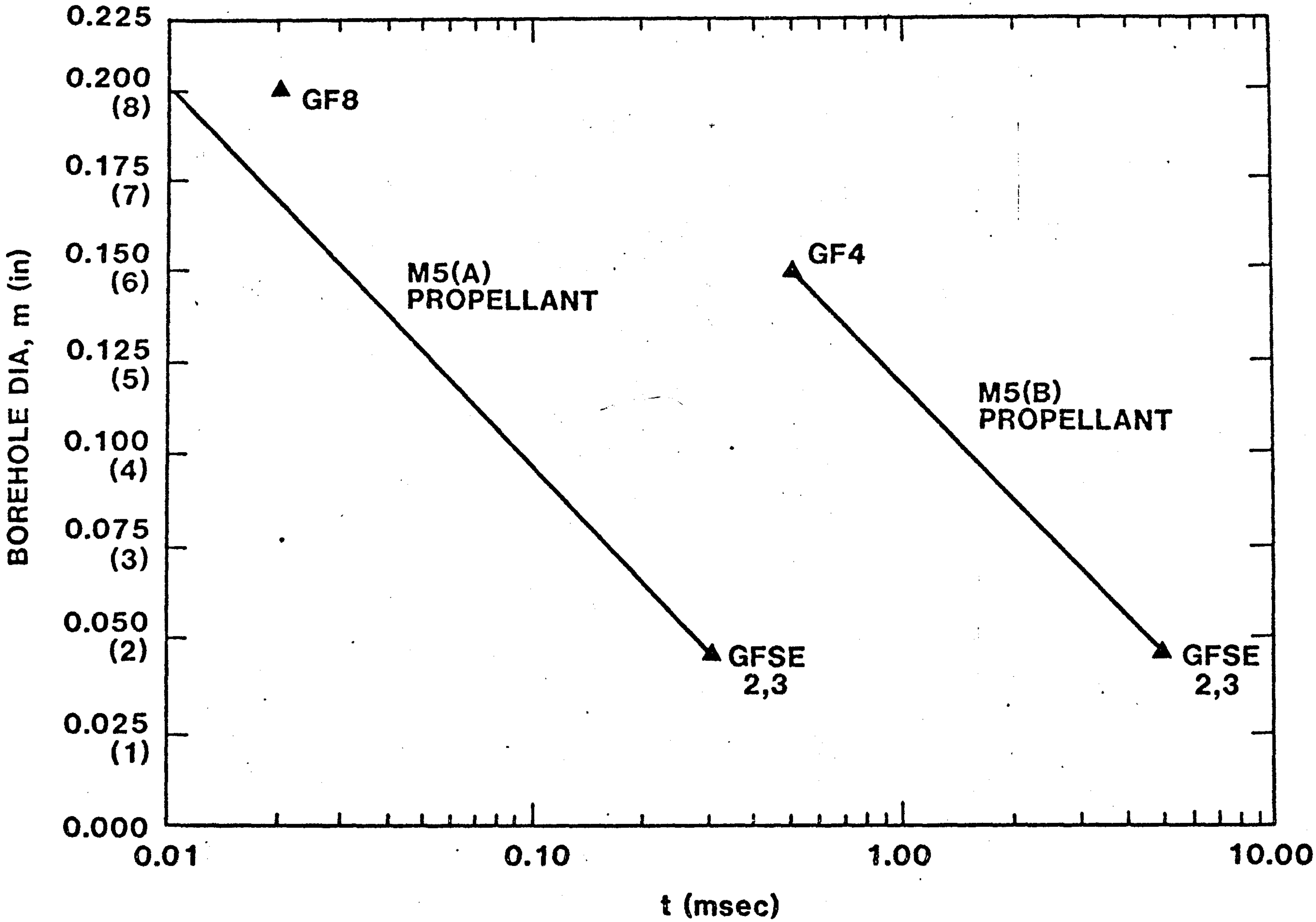

BOREHOLE DIA, m (in)
0.225
0.200 (8)
0.175 (7)
0.150 (6)
0.125 (5)
0.100 (4)
0.075 (3)
0.050 (2)
0.025 (1)
0.000
0.01
0.10
1.00
10.00
t (msec)
GF8
M5(A) PROPELLANT
GF4
M5(B) PROPELLANT
GFSE 2,3
GFSE 2,3


FIG 6